Organic & Biomolecular Chemistry

Cite this: *Org. Biomol. Chem.*, 2011, **9**, 3530

www.rsc.org/obc

PAPER

Synthesis and evaluation of self-calibrating ratiometric viscosity sensors†

Hyung-Jo Yoon,[a] Marianna Dakanali,[a] Darcy Lichlyter,[b] Willy M. Chang,[a] Karen A. Nguyen,[a] Matthew E. Nipper,[b] Mark A. Haidekker*[b] and Emmanuel A. Theodorakis*[a]

Received 18th November 2010, Accepted 21st February 2011
DOI: 10.1039/c0ob01042a

We describe the design, synthesis and fluorescent profile of a family of self-calibrating dyes that provide ratiometric measurements of fluid viscosity. The design is based on covalently linking a primary fluorophore (reference) that displays a viscosity-independent fluorescence emission with a secondary fluorophore (sensor) that exhibits a viscosity-sensitive fluorescence emission. Characterization of fluorescent properties was made with separate excitation of the units and through Resonance Energy Transfer from the reference to the sensor dye. The chemical structures of both fluorophores and the linker length have been evaluated in order to optimize the overall brightness and sensitivity of the viscosity measurements. We also present an application of such ratiometric dyes for the detection of membrane viscosity changes in a liposome model.

Introduction

A number of functions and diseases at the cellular[1] and organismal level[2] are related to alterations in the fluid viscosity. For example, cell membrane viscosity depends on the chemical composition of the bilayer, and its variations alter the function of various membrane-bound enzymes and receptors.[3] In turn, this leads to disorders such as cardiovascular disease,[4] cell malignancy,[5] and Alzheimer's disease.[6] In a similar manner, changes of viscosity at the organismal level (*e.g.* blood, plasma or lymphatic fluids) have been linked to diabetes,[7] hypertension,[8] infarction,[9] and aging.[10]

The increasing interest in quantifying membrane viscosity in cellular biology and physiology has led to the development of a variety of methods for its precise measurement. The well known cone-and-plate viscometers and capillary viscometers,[11] are limited by the need for large sample size and are not effective in measuring viscosity changes in real-time.[12] On the other hand, fluorescent based viscosity measurements have gained advantage due to the rapid response time and good spatial resolution of the fluorescent probes.[13] In fact, microviscosity changes in cells can predominantly be measured using fluorescence-based methods. Specifically, techniques such as fluorescence anisotropy[14] and fluorescence recovery after photobleaching[15] are commonly used in biological systems. Despite their common use, such techniques suffer from the need for specialized instruments, high energy light and limited spatial resolution.[16]

An alternative method for measuring viscosity is based on a class of environment-sensitive fluorescent probes.[17] Referred to as molecular rotors, these probes are known to form twisted intramolecular charge transfer (TICT) complexes in the excited state producing a fluorescent quantum yield that is dependent of the surrounding environment.[18] Common to the structure of all molecular rotors is a motif that consists of an electron donor group in π-conjugation with an electron acceptor group. Following photoexcitation, this motif has the unique ability to relax either *via* fluorescence emission or *via* an internal non-radiative process that involves molecular rotation between the donor and the acceptor. When this rotation is hindered due to the high viscosity of the environment, the relaxation occurs *via* an increased fluorescence emission. In contrast, in solvents of low viscosity the relaxation proceeds mainly *via* a non-radiative pathway. Fig. 1 shows representative structures of molecular rotors. Modifications in the π-conjugation system, the donor or the acceptor affect significantly the fluorescence profile of such molecules.[19]

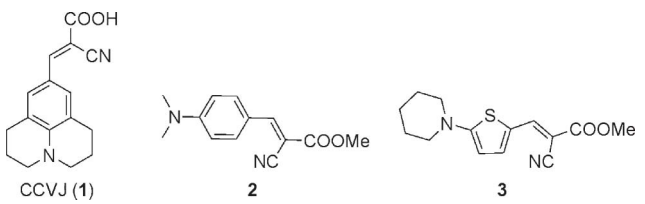

Fig. 1 Chemical structures of representative molecular rotors.

Fluorescent molecular rotors have been used for viscosity studies that are performed by steady-state fluorescence through emission intensity measurements. This method, however, is sensitive to changes of the fluid optical properties and to dye concentrations. Some molecular rotors, most notably

[a]*Department of Chemistry & Biochemistry, University of California, San Diego, 9500 Gilman Drive MC: 0358, La Jolla, CA 92093-0358, USA. E-mail: etheodor@ucsd.edu; Fax: +1-858-822-0386; Tel: +1-858-822-0456*
[b]*Faculty of Engineering, University of Georgia, Athens, GA 30602, USA*

† Electronic supplementary information (ESI) available: ^{1}H and ^{13}C NMR and fluorescence spectra for all compounds. Experimental procedures for the synthesis of compounds, **5**, **6**, **8** and **9**. See DOI: 10.1039/c0ob01042a

4,4-dimethylaminobenzonitrile (DMABN), exhibit dual fluorescence and it has been proposed to use the isosbestic point of such dual emission as a calibration intensity.[20] However, emission from the twisted state strongly depends on solvent polarity, excimer formation, and hydrogen bond formation.[21] A more promising approach is to choose a reference fluorophore and covalently bind it to a molecular rotor, forming a self-calibrating dye system. Single-emission molecular rotors generally obey a power-law relationship between quantum yield Φ_F and viscosity η, namely,

$$\Phi_F = C\eta^x \quad (1)$$

where, C is a dye-dependent constant and x depends on dye-solvent interaction.[18a] Additional factors, such as excitation intensity I_{EX}, dye concentration c and instrument gain factors G determine the steady-state intensity I_{EM}:

$$I_{EM} = GcI_{EX}\Phi_F = (GcI_{EX}C)\eta^x \quad (2)$$

With a ratiometric dye system, a second, viscosity-independent emission, I_{REF}, becomes available that is proportional to the same factors except for the reference quantum yield Φ_{REF}, which is viscosity-independent. The reference emission serves as the internal calibration emission. The ratio of rotor emission and reference emission therefore simplifies to:

$$\frac{I_{EM}}{I_{REF}} = \frac{C}{\Phi_{REF}}\eta^x \quad (3)$$

which explains the self-calibrating nature of these engineered dyes. One example of such a ratiometric dye is compound **4** (Fig. 2), in which a viscosity-sensitive molecular rotor (dimethylaminobenzylidine motif in Fig. 2) has been linked to a reference dye (coumarin motif in Fig. 2), which exhibited no viscosity sensitivity.[22]

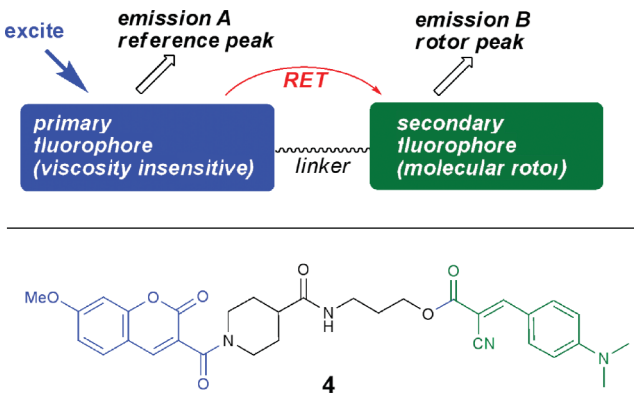

Fig. 2 General design of a ratiometric self-calibrating viscosity sensor.

The design of an appropriate self-calibrating ratiometric viscosity sensor requires optimization of the resonance energy transfer (RET) between the two dyes. In turn, this indicates that the optical properties of the two dyes and their spatial distance should be evaluated. Herein, we report the synthesis and fluorescence properties of a number of ratiometric dyes that are formed by covalently linking different molecular rotors with coumarins. We have evaluated the effect of the dye structure and the size of the linker to the viscosity measurements in a representative mixture of organic solvents (ethylene glycol : glycerol). We also demonstrate the efficacy of such ratiometric dye in a model phospholipid bilayer.

Results and discussion

Design criteria of a ratiometric self-calibrating dye

The general design of a ratiometric self-calibrating viscosity dye is shown in Fig. 2 and involves covalent linking of two fluorophores, one acting as an internal reference and the other being a molecular rotor. These two fluorophores should form a resonance energy transfer pair which implies that: (a) the emission spectrum of the primary fluorophore should have a significant overlap with the excitation spectrum of the secondary fluorophore and (b) that the two fluorophores are kept within a distance approximately equal to the Förster radius.[13,23] To facilitate the measurements, the primary fluorophore should be a viscosity insensitive dye (reference dye) with a high but constant fluorescence emission quantum yield that can sufficiently excite the molecular rotor (viscosity sensitive dye). Following excitation of the reference dye, the ratio of the emission A to emission B should then produce a concentration-independent self-calibrating measurement of the solvent viscosity. Compound **4** highlights this design.[22]

Previous studies from our group indicated that the *N*,*N*-dimethyl aniline- and amino thiophene-containing dyes, such as compounds **2** and **3** (Fig. 1), have excellent properties as viscosity dyes that include very good viscosity sensitivity and significant brightness.[19] With the above design in mind we decided to use the thiophene or dimethylaminobenzylidine motif as the secondary fluorophore. We envisioned that as the primary fluorophore, a coumarin donor with the appropriate emission wavelength could be used. To fine-tune its optical properties we selected coumarins **5**, **6** and **7** (Fig. 3). Finally, to connect the two fluorophores we chose a polymethylene linker of variable length.

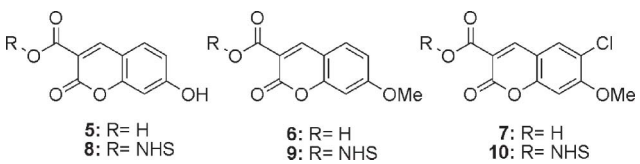

Fig. 3 Chemical structures of coumarins used as reference dyes.

Synthesis of coumarins

The synthesis of the new coumarin **10** is illustrated in Scheme 1. Chlororesorcinol **11** was converted to monomethylated compound **12** in 67% overall yield *via*: (a) tosylation of the less sterically hindered hydroxyl group followed by methylation of the second hydroxyl group; and (b) hydrolysis of the tosylate.[24] Formylation of **12** using $MgCl_2$ and *p*-formaldehyde under basic conditions formed benzaldehyde **13** (61% yield).[25] Treatment of **13** with Meldrum's acid (**14**) in the presence of catalytic amounts of piperidine produced coumarin **7**, which was converted to the activated NHS-ester **10** upon esterification using EDC (64% combined yield).

The synthesis of coumarins **8** and **9** was achieved, according to the literature,[26] starting from the appropriate benzaldehydes and repeating steps (d) and (e) of Scheme 1. The combined yields were 53% and 74% respectively.

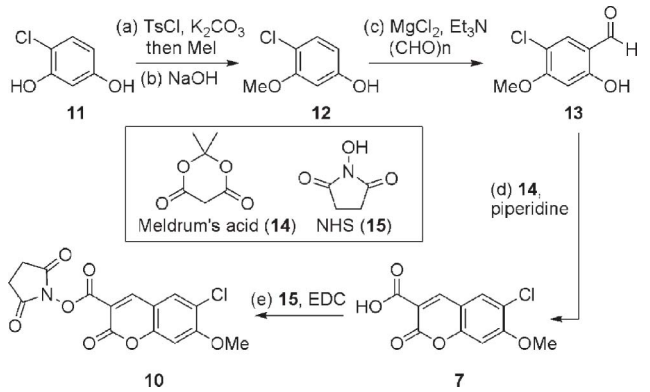

Scheme 1 *Reagents and conditions*: (a) 1.0 equiv. **11**, 1.1 equiv. TsCl, 3.0 equiv. K_2CO_3, acetone, 18 h, reflux, then 2.0 equiv. MeI, 18 h, reflux, 76%; (b) 5.0 equiv. NaOH 2 M, methanol, 4 h, reflux, 88%; (c) 1.0 equiv. **12**, 2.0 equiv. $MgCl_2$, 2.0 equiv. Et_3N, 3.0 equiv. $(CHO)_n$, THF, 18 h, reflux, 61%; (d) 1.0 equiv. **13**, 1.0 equiv. **14**, 0.1 equiv. piperidine, EtOH, 24 h, reflux, 84%; (e) 1.0 equiv. **7**, 1.0 equiv. **15**, 1.1 equiv. EDC, DMF, 18 h, 40 °C, 76%.

Synthesis of ratiometric dyes

The synthesis of the ratiometric dyes containing the aminothiophene rotor is highlighted in Scheme 2. Commercially available aldehyde **16** was converted to the piperidine derivative **17** in 97% yield.[27] Knoevenagel condensation of **17** with the various β-cyanoesters **20a–d** gave compounds **21a–d** in very good yields.[19] Deprotection of the primary amines **21a–d**, followed by coupling with the activated coumarin **9**, yielded the final ratiometric dyes **23a–d**. The length of the linkers and the yields of the final products are shown in Table 1.

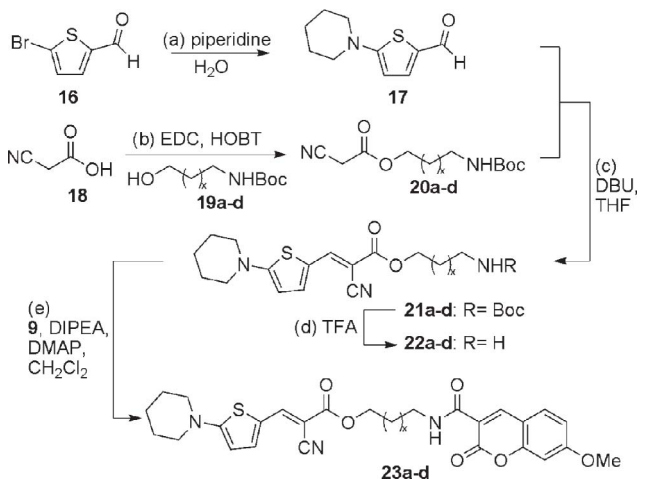

Scheme 2 *Reagents and conditions*: (a) 1.0 equiv. **16**, 1.1 equiv. piperidine, H_2O, 18 h, reflux, 97%; (b) 1.0 equiv. **18**, 1.0 equiv. **19**, 1.0 equiv. EDC, 1.0 equiv. HOBT, CH_2Cl_2, 6 h, 25 °C, 70–98%; (c) 1.0 equiv. **17**, 1.1 equiv. **20**, 1.16 equiv. DBU, THF, 18 h, 25 °C, 70–95%; (d) 1.0 equiv. **21**, TFA/CH_2Cl_2, 30 min, 25 °C; (e) 1.1 equiv. **22**, 1.0 equiv. **9**, 2.0 equiv. DIPEA, 0.1 equiv. DMAP, CH_2Cl_2, 18 h, 25 °C, 52–79% (over two steps).

In a similar manner, the ratiometric dyes **27a–d** were synthesized, as depicted in Scheme 3. Knoevenagel condensation of the commercially available *N*,*N*-dimethylamino benzaldehyde **24** with **20a–d** gave rise to the molecular rotors **25a–d**.[19] Deprotection

Table 1 Structures and yields for ratiometric dyes

Cmp #	Number of carbons in linker	Rotor	Coumarin	Yield (%)
23a	3	**3**	**6**	61
23b	5	**3**	**6**	63
23c	6	**3**	**6**	70
23d	8	**3**	**6**	52
27a	3	**2**	**6**	69
27b	5	**2**	**6**	74
27c	6	**2**	**6**	64
27d	8	**2**	**6**	78
28	3	**2**	**5**	53
29	3	**2**	**7**	97

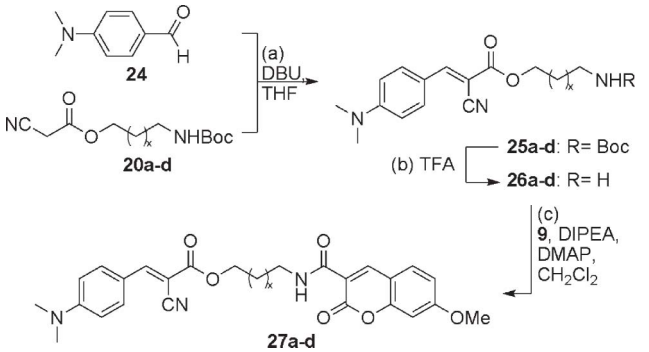

Scheme 3 *Reagents and conditions*: (a) 1.0 equiv. **24**, 1.1 equiv. **20**, 1.16 equiv. DBU, THF, 18 h, 25 °C, 62–82%; (b) 1.0 equiv. **25**, TFA/CH_2Cl_2, 30 min, 25 °C; (c) 1.1 equiv. **26**, 1.0 equiv. **9**, 2.0 equiv. DIPEA, 0.1 equiv. DMAP, CH_2Cl_2, 18 h, 25 °C, 64–78% (over two steps).

of the primary amines **25a–d** and coupling with the coumarin **9** resulted the aniline containing dyes **27a–d**. The length of the linkers and the yields of the final products are shown in Table 1.

The ratiometric dyes **28** and **29** (Fig. 4) were synthesized by adapting the above experimental procedures to the appropriate coumarin and/or molecular rotor.

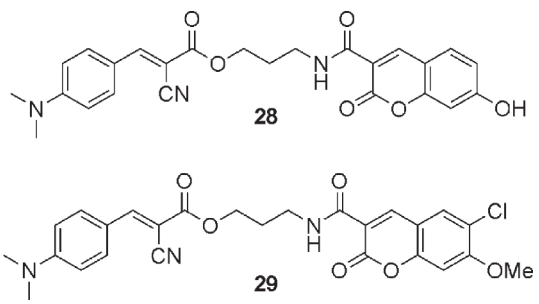

Fig. 4 Chemical structures of molecular rotors **28** and **29**.

Fluorescence properties of ratiometric dyes

Representative emission spectra of **23a**, **27a**, recorded *via* RET or direct excitation are shown in Fig. 5. All dyes exhibited dual emission consistent with earlier work, as shown by the peaks of Fig. 5a and 5d.[22] The peaks with emission maxima around 400 nm and 490 nm correspond to the coumarin (donor) and the rotor (acceptor) motif, respectively. The emission spectra of the rotor motif of probes **23a** and **27a** under direct excitation are shown in Fig. 5b and 5e respectively. The viscosity sensitivity

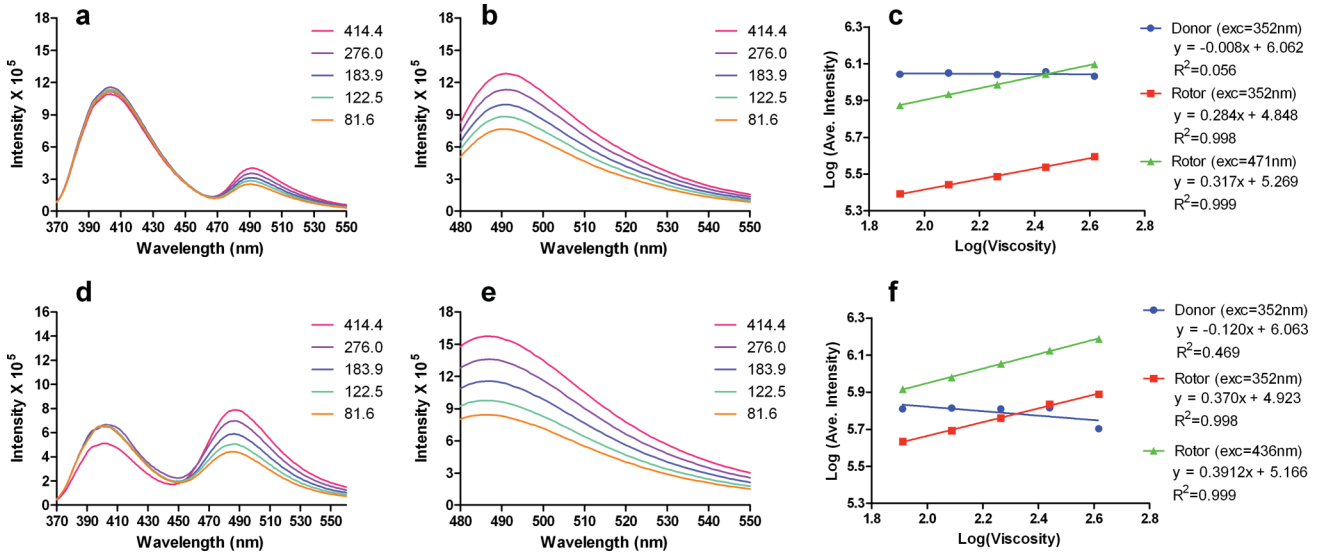

Fig. 5 Fluorescence emission spectra and viscosity sensitivity plots of ratiometric rotors **23a** (Fig a, b, c) and **27a** (Fig. d, e, f) in ethylene glycol : glycerol mixtures (viscosity is recorded in mPa·s). Fig. a: emission spectra *via* RET (exc = 352 nm); Fig. d: emission spectra *via* RET (exc = 352 nm); Fig. b: emission spectra under direct excitation of the rotor motif (exc = 471 nm); Fig. e: emission spectra under direct excitation of the rotor motif (exc = 436 nm); Fig. c, f: viscosity sensitivity plots.

Table 2 Fluorescent properties and viscosity sensitivity of the donor peak

Compound #	Exc λ (nm)	Em λ (nm)	Power-law slope of donor	y-intercept (10^6 cps)
23a	352	404	–0.008	1.15
23b	352	403	0.020	1.66
23c	353	404	–0.025	4.4
23d	352	402	–0.017	4.55
27a	352	400	–0.120	1.16
27b	355	398	–0.075	1.05
27c	355	400	–0.081	0.66
27d	355	398	0.088	0.29
28	357	404	–0.032	1.44
29	357	404	–0.192	0.73

profiles of compounds **23a** and **27a** are shown in Fig. 5c and 5f respectively.

Detailed spectroscopic data for all compounds are given in Tables 2 and 3. In all cases, the coumarin (donor) was excited near 355 nm (see Table 2, column 2) and emitted around 400 nm (see Table 2, column 3). The molecular rotor subunit, excited either directly or indirectly from the donor unit through RET, emits near 480–490 nm (see Table 3, column 3). The y-intercept in Tables 2 and 3 combines the proportionality constants G, C, I_{EM} and c from eqn (2) and provides information about the overall brightness of the dye.[18a,19] The columns labeled *viscosity sensitivity* (Table 3) refer to the exponent x in eqn (1)–(3) and give a measure of how much the rotor intensity increases with increased viscosity. The exponent x can be obtained by plotting peak emission intensity over the viscosity in a double logarithmic scale, where x is the slope of the regression line. Fluorescence emission spectra and viscosity sensitivity plots of all ratiometric rotors are shown in the ESI.†

Comparison of the spectroscopic data of Fig. 5 leads to the following general observations:

i. In all cases, the donor fluorescence was viscosity-independent between 81–276 mPa·s. However, a small drop in intensity was observed for solvent viscosity of 414.4 mPa·s This is more evident in Fig. 5d. This drop may be due to reduced solubility of these probes in increased glycerol content.

ii. Under direct excitation, the y-intercept of the rotor fluorophore was higher in all cases than when excited through RET (Fig. 5a/b and d/e). This is evident by comparing columns 5 and 7 in Table 3. This is explained by considering that excitation through RET is less efficient than direct excitation.

Table 3 Fluorescent properties and viscosity sensitivity of the rotor peak

Cmp#	Exc λ (nm)	Em λ (nm)	Viscosity sensitivity with donor exc λ	y-intercept (donor exc, 10^6 cps)	Viscosity sensitivity with rotor exc λ	y-intercept (rotor exc, 10^6 cps)
23a	471	491	0.284	0.07	0.317	0.19
23b	470	491	0.321	0.11	0.356	0.29
23c	469	494	0.314	0.22	0.347	0.44
23d	470	493	0.289	0.31	0.321	0.57
27a	436	486	0.371	0.08	0.391	0.13
27b	437	487	0.419	0.14	0.430	0.22
27c	437	486	0.441	0.1	0.427	0.19
27d	437	485	0.307	0.32	0.389	0.34
28	434	487	0.358	0.14	0.366	0.25
29	436	482	0.299	0.06	0.349	0.1

Table 4 Extrapolated ratiometric intensities at $\eta = 1$ mPa·s

Compound #	I_{Em}/I_{ref} (donor exc)	I_{Em}/I_{ref} (rotor exc)
23a	0.06	0.16
23b	0.07	0.17
23c	0.05	0.1
23d	0.07	0.12
27a	0.07	0.11
27b	0.13	0.21
27c	0.15	0.29
27d	1.10	1.17
28	0.10	0.17
29	0.08	0.14

iii. Upon RET excitation the brightness of the acceptor is smaller for the thiophene-containing compound **23a** (Fig. 5a) than for the aniline dye **27a** (Fig. 5d). This can be explained due to the inefficient excitation of the thiophene dye from the coumarin. Specifically, for **23a** the λ_{max} of the coumarin emission is 404 nm while the λ_{max} for the thiophene excitation is 470 nm. On the other hand, in **27a** the excitation maximum for the aniline dye is 436 nm allowing a more efficient resonance energy transfer, which translates to higher intensity. This observation is consistent with all fluorophores as shown in Table 3, column 5.

iv. To better compare intensities, we use the extrapolated intensity at a viscosity of 1 mPa·s, shown as the *y*-intercept in Tables 2 and 3. Under direct excitation, the thiophene fluorophore is brighter than aniline, which is in accordance with previous results.[19] At higher viscosities (Fig. 5b/e), the aniline-based rotor increases its intensity over that of the thiophene-based rotor because of its higher sensitivity.

v. The sensitivity of the aniline-based dye **27a** (Fig. 5f) was slightly better than that of the thiophene-containing sensor **23a** (Fig. 5c) both when the chromophore was excited through RET or directly excited. This is also shown in Table 3 columns 4 and 6, respectively.

For the design of an optimum ratiometric dye, the sensor (rotor) peak should be as high, or higher, than the reference peak to achieve a good signal-to-background ratio. This is particularly important for low viscosities, where the rotor emission is naturally low. The length of the linker is one factor that influences dye brightness, and Table 4 shows the ratiometric intensities as the extrapolated viscosity of 1 mPa·s for all dyes.

In the thiophene-containing dyes **23a–23d** the coumarin (donor) intensity increased by increasing the linker length (Table 2, column 5). In particular with linkers of 6 and 8 carbons (compounds **23c** and **23d**), the intensity of the reference peak increased more strongly with increasing linker length than that of the rotor peak and therefore led to a decrease of the ratiometric intensity. In contrast, when the aniline rotor was used (compounds **27a–d**), the donor intensity decreased upon increasing the length of the linker, making **27a–d** more attractive as self-calibrating dyes in high-viscosity environments.

Table 4 highlights the influence of the linker length on the balance between reference and rotor emission. The ratiometric intensities in Table 4 are extrapolated to a viscosity of 1 mPa·s (*i.e.*, *y*-intercept of the log–log plot) for better comparison. It can be seen that the ratiometric intensity increases with the linker length in the aniline-based molecules. Noticeably, in the thiophene-containing dyes the ratiometric intensity, when excited through RET, remains approximately constant.

The fluorescent properties of the coumarin donor can be modified as a function of its substitution. For instance, it has been proposed that hydroxylation and/or halogenation of the coumarin motif increases its quantum yield and induces a fluorescence bathochromic shift.[28,29] With this in mind, we evaluated compounds **28** and **29** containing the 7-hydroxy-coumarin and the 6-chloro-7-methoxy-coumarin, respectively. The fluorescent properties of these dyes are shown in Fig. 6 and Tables 2 and 3.

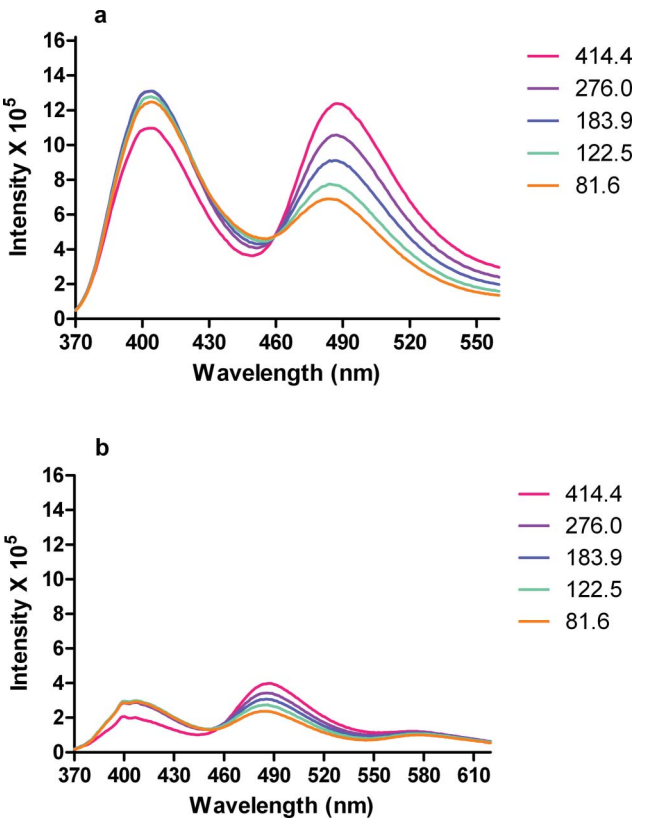

Fig. 6 Fluorescence emission spectra of ratiometric rotors **28** (Fig a) and **29** (Fig. b). The spectra were acquired at λexc = 357 nm in ethylene glycol : glycerol mixtures (viscosity is recorded in mPa·s).

Comparison of **28** with **27a** indicates that replacement of the methoxy unit by a hydroxyl group results in a decrease of the viscosity sensitivity and does not induce any significant emission shift in the fluorescence profile of the dye. Moreover, compound **28** proved to be sensitive to changes of pH and solvent polarity. This is in agreement with literature reports on simple hydroxy coumarins.[29b] Similarly, comparison of **29** with **27a** indicates that addition of a chloro group to a methoxycoumarin results in a decrease of the viscosity sensitivity and dye brightness and does not induce any significant emission shift in the fluorescence profile of the dye. These observations indicate that the methoxy coumarin motif is more appropriate as the donor fluorophore.

Viscosity measurements in liposomes using ratiometric dyes

In a DLPC (DiLauroylPhosphatidylCholine) liposome model, we examined the change of the ratiometric emission intensity

when the liposomes were exposed to propanol. Alcohols are known to reduce membrane viscosity at low concentrations in aqueous environments, and propanol has a very high interfacial energy with respect to the membrane.[30] As propanol intercalates with the polar headgroups, the free-volume increases within the membrane resulting in a lower microviscosity. Such a decrease in microviscosity would be directly responsible for a decrease in emission intensity of the rotor.

Intrigued by the observation that in the thiophene-containing dyes **23a–d** the ratiometric intensity is independent of the linker length, we decided to evaluate their viscosity sensitivity in the DLPC model. As propanol is added to a liposome suspension that is labeled with a ratiometric dye, the rotor intensity is expected to decrease, as is the ratiometric intensity (eqn (3)). This decrease, normalized to non-propanol controls, is shown in Fig. 7. A lower value in the bar graph indicates a stronger decrease and therefore a stronger response. We observed that the change of the ratiometric intensity depends on the size of the linker that joins the two dye molecules: a shorter linker shows a larger decrease of the ratiometric intensity with the addition of propanol than a longer linker, although the amount of propanol (and therefore its effect on the membrane) remains the same. We conclude that dyes with a shorter linker are more sensitive reporters for microviscosity in this context.

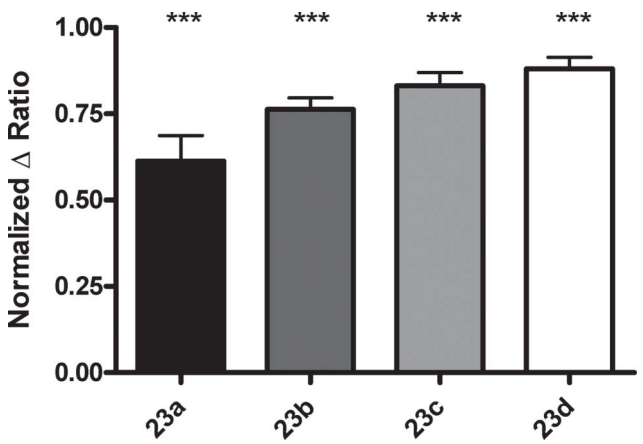

Fig. 7 Sensitivity of dyes **23a–d** when reporting membrane viscosity changes in DLPC giant unilamellar vesicles. Vesicles were exposed to 5% propanol in an aqueous environment, and the change of the ratiometric intensity as a consequence of propanol exposure was recorded. Dyes with shorter linkers (notably, **23a**), exhibit a stronger relative change of intensity than dyes with longer linkers. Bars represent mean values from $n = 10$ independent experiments, and the error bars represent standard deviation. All mean values are significantly different ($P < 0.0001$, ***) from all other means, tested by one-way ANOVA.

There are two possible explanations for this observation. First, it is possible that a shorter linker leads to increased resonance energy transfer efficiency with the consequence of a larger rotor emission and a higher signal-to-background ratio. With shorter linkers, changes in the rotor emission are more pronounced. Another possible explanation for this increased response is specific localization within the membrane. The more hydrophobic dyes, such as **23d** may target the inner regions of the membrane, where van der Waals forces dominate and the effect of alcohol is reduced. Conversely, dyes with a shorter linker, such as **23a**, localize closer to the surface where the effect of propanol on the polar phospholipid regions is largest.

Conclusions

We present here a study toward the design and development of self-calibrating fluorescent sensors that can be used for ratiometric measurements of viscosity. The design is based on covalently linking a reference fluorophore (donor) with a molecular rotor (acceptor). The reference fluorophore has a viscosity independent fluorescence emission, while the emission of the molecular rotor is viscosity-dependent. The chemical structures of both dyes and the linker length were evaluated in order to optimize the resonance energy transfer between the two fluorophores. Among the coumarin structures that we examined as primary fluorophores, the 7-methoxy coumarin motif was found to be most adequate as the reference dye, due to its overall environment insensitivity, accessibility and appropriate fluorescent profile. As acceptors either the *N*,*N*-dimethyl aniline or the amino thiophene motifs can be used. In mixtures of ethylene glycol/glycerol, the *N*,*N*-dimethyl aniline motif had a more efficient resonance energy transfer from the reference dye, producing a brighter fluorescent signal. We also evaluated the thiophene family of ratiometric dyes in a DLPC model. The results show that shorter linker length produces a more viscosity sensitive dye. This design can be applied to the development of dyes for microviscosity and free volume measurements in various environments.[31]

Experimental

General notes. All reagents were purchased at highest commercial quality and used without further purification except where noted. DPLC was purchased from Avanti Polar lipids. Air- and moisture-sensitive liquids and solutions were transferred *via* syringe or stainless steel cannula. Organic solutions were concentrated by rotary evaporation below 45 °C at approximately 20 mmHg. All non-aqueous reactions were carried out under anhydrous conditions. Yields refer to chromatographically and spectroscopically (^{1}H NMR, ^{13}C NMR) homogeneous materials, unless otherwise stated. Reactions were monitored by thin-layer chromatography (TLC) carried out on 0.25 mm Dynamic Adsorbents, Inc. silica gel plates (60F-254) and visualized under UV light and/or developed by dipping in solutions of 10% ethanolic phosphomolybdic acid (PMA) and applying heat. Dynamic Adsorbents, Inc. silica gel (60, particle size 0.040–0.063 mm) was used for flash chromatography. NMR spectra were recorded on the Varian Mercury 400, 300 and/or Unity 500 MHz instruments and calibrated using the residual non-deuterated solvent as an internal reference. The following abbreviations were used to explain the multiplicities: s = singlet, d = doublet, t = triplet, q = quartet, m = multiplet, b = broad. IR spectra were recorded on a Nicolet 320 Avatar FT-IR spectrometer, and values are recorded in cm^{-1} units. High resolution mass spectra (HRMS) were recorded on a VG 7070 HS mass spectrometer under electron spray ionization (ESI) or electron impact (EI) conditions.

4-Chloro-3-methoxyphenol (12)[24]. To a solution of 4-chlororesorcinol (**11**) (5 g, 34.6 mmol) in anhydrous acetone (494 ml), *p*-toluenesulfonyl chloride (7.25 g, 38.0 mmol) and

potassium carbonate (14.3 g, 103 mmol) were added. The suspension was heated under reflux overnight. Iodomethane (9.8 g, 69.2 mmol) was added to the suspension after being cooled to room temperature. The reaction was heated at 70 °C overnight. The inorganic solids were filtered out and the filtrate was concentrated under reduced pressure. The residue was then dissolved in water and extracted with ethyl acetate (3 × 50 ml), washed with water (30 ml) and brine (30 ml). The organic layer was dried over $MgSO_4$ and purified by column chromatography (10–30% EtOAc–hexanes). To a round bottom flask, NaOH (60 ml, 2 N) was then added to a solution of 2-chloro-5-(toluene-4-sulfonyloxy) anisole (313 mg, 26.16 mmol) in methanol (304 ml). The suspension was heated to reflux for 5 h and upon completion was concentrated and neutralized with HCl (1 N). The product was extracted with DCM (3 × 100 ml) and the organic layer was washed with water (100 ml) and brine (100 ml), dried over $MgSO_4$ and concentrated to yield **12** (3.76 g, 90%). **12**: yellow solid; ^{1}H NMR (400 MHz, $CDCl_3$) δ 7.18 (d, 1H, J = 8.5 Hz), 6.47 (d, 1H, J = 2.7 Hz), 6.35 (dd, 1H, J = 2.7 Hz, J = 8.5 Hz), 3.87 (s, 3H); ^{13}C NMR (100 MHz, $CDCl_3$) δ 155.5, 155.2, 130.3, 113.8, 108.0, 100.6, 55.0; HRMS calc for $C_7H_7ClO_2$ $(M)^+$ 158.0129 found 158.0130.

5-Chloro-2-hydroxy-4-methoxybenzaldehyde (13)[25]. To a round bottom flask, magnesium chloride (4.40 g, 46.25 mmol), triethylamine (6.45 ml, 46.25 mmol), and paraformaldehyde (2.08 g, 69.37 mmol) were added to a solution of 4-chloro-3-methoxyphenol (**12**) (3.67 g, 23.12 mmol) in dry THF (230 ml). The reaction was refluxed overnight at 85 °C and upon completion and cooling to room temp., it was diluted with ether, washed with HCl (1 N, 2 × 200 ml), and water (2 × 200 ml). The organic layer was dried over $MgSO_4$, concentrated under reduced pressure and purified by column chromatography (5–20% EtOAc–hexane) to yield **13** (2.72 g, 62%). **13**: yellow solid; ^{1}H NMR (400 MHz, $CDCl_3$) δ 11.36 (bs, 1H), 9.61 (m, 1H), 7.42 (s, 1H), 6.41 (s, 1H), 3.89 (s, 3H); ^{13}C NMR (100 MHz, $CDCl_3$) δ 193.6, 162.8, 161.5, 133.7, 114.7, 114.0 100.2, 56.5; HRMS calc for $C_8H_7ClO_3$ $(M)^+$ 186.0078 found 186.0079.

3-Carboxy-6-chloro-7-methoxycoumarin (7). To a round bottom flask, Meldrum's Acid (228 mg, 1.58 mmol) was added to a solution of 5-chloro-2-hydroxy-4-methoxy benzaldehyde (**13**) (295 mg, 1.58 mmol) in ethanol (5 ml). Piperidine (20 µl, 0.158 mmol) was then added to the resulting solution and stirred for 20 min at room temperature. The reaction was heated to reflux overnight. Upon completion, the reaction was cooled to 0 °C and the product was filtered out and washed with cold ethanol, (338 mg, 84%). **17**: off-white solid; ^{1}H NMR (400 MHz, DMSO-d_6) δ 8.66 (s, 1H), 8.05 (s, 1H), 7.27 (s, 1H), 3.98 (s, 3H); ^{13}C NMR (100 MHz, DMSO-d_6) δ 164.0, 159.1, 156.7, 155.5, 147.7, 130.1, 118.1, 112.0, 100.7, 57.4; IR (film) ν_{max} 2838, 1753, 1678, 1604, 1174; HRMS calc for $C_{11}H_7ClO_5Na$ $(M+Na)^+$ 276.9874 found 276.9876.

3-Carboxy-6-chloro-7-methoxycoumarin succinimidyl ester (10). To a round bottom flask, *N*-hydroxysuccinimide (136 mg, 1.18 mmol) and EDC·HCL (249 mg, 1.30 mmol) were added to a stirred suspension of 6-chloro-7-methoxy-3-carboxycoumarin (**7**) (300 mg, 1.18 mmol) in DMF (3 ml) at room temperature. The reaction was heated overnight at 40 °C. Upon completion, the reaction was quenched with 10% citric acid solution (10 ml) and washed with ethyl acetate (3 × 30 ml). The product was isolated by filtration (316 mg, 76%) **10**: pale yellow, green solid; R_f 0.44 (3% MeOH in CH_2Cl_2); ^{1}H NMR (400 MHz, DMSO-d_6) δ 9.03 (s, 1H), 8.17 (s, 1H), 7.33 (s, 1H), 4.02 (s, 3H), 2.89 (s, 4H); ^{13}C NMR (100 MHz, DMSO-d_6) δ 170.3, 160.6, 158.4, 156.6, 155.2, 151.8, 131.1, 118.6, 111.7, 109.1, 100.9, 57.7, 25.5; IR (film) ν_{max} 1727, 1599, 1196; HRMS calc for $C_{15}H_{10}NClO_7Na$ $(M+Na)^+$ 374.0038 found 374.0040.

***tert*-Butyl(8-hydroxyoctyl)carbamate (19d).** Di-*tert*-butyl dicarbonate (609 mg, 2.79 mmol) was added to a solution of 8-amino-1-octanol (200 mg, 1.38 mmol) in a 9 : 1 (v/v) mixture of methanol/triethylamine (13 ml). The reaction was left stirring under reflux and upon completion, the solvent was removed under reduced pressure and the residue extracted with DCM/water. The organic layer was dried over anhydrous Na_2SO_4 and concentrated under reduced pressure to yield **19d** (304 mg, 90%). **19d**: yellow oil; R_f 0.17 (2% MeOH in CH_2Cl_2); ^{1}H NMR (400 MHz, $CDCl_3$) δ 4.92 (bs, 1H), 3.41 (t, 2H, J = 6.7 Hz), 3.34 (bs, 1H), 2.91 (m, 2H), 1.37 (m, 2H), 1.26 (s, 10H), 1.14 (s, 9H); ^{13}C NMR (100 MHz, $CDCl_3$) δ 156.0, 78.9, 62.7, 40.5, 32.6, 29.9, 29.2, 29.1, 28.3, 26.6, 25.6; HRMS calc for $C_{13}H_{27}NO_3Na$ $(M+Na)^+$ 268.1883 found 268.1884.

General procedure for the preparation of β-cyanoacetate 20. To a round bottom flask containing a solution of the BOC-protected amino alcohol **19** (5.41 mmol) and cyanoacetic acid (3.44 mmol) in 10 ml of anhydrous DCM, EDC (5.43 mmol) and HOBT (5.43 mmol) were added. The formation of the product was monitored by TLC and was completed after overnight stirring at room temperature. The crude mixture was concentrated under reduced pressure and the product was purified *via* flash chromatography (10–30% EtOAc–hexanes).

β-Cyanoacetate 20a. 68% yield; yellow oil; R_f 0.5 (2% MeOH in CH_2Cl_2); ^{1}H NMR (400 MHz, $CDCl_3$) δ 4.81 (s, 1H), 4.22 (t, 2H, J = 6.2 Hz), 3.47 (s, 2H), 3.16 (m, 2H), 1.81 (m, 2H), 1.38 (s, 9H); ^{13}C NMR (100 MHz, $CDCl_3$) δ 163.0, 155.9, 113.0, 79.2, 64.1, 36.8, 28.7, 28.2, 24.6; IR (film) ν_{max} 3367, 2976, 2202, 1745, 1689, 1248, 1162; HRMS calc for $C_{11}H_{18}N_2O_4Na$ $(M+Na)^+$ 265.1159 found 265.1163.

β-Cyanoacetate 20b. 33% yield; yellow oil; R_f 0.5 (2% MeOH in CH_2Cl_2); ^{1}H NMR (400 MHz, $CDCl_3$) δ 4.69 (bs, 1H), 4.12 (t, 2H, J = 6.6 Hz), 3.43 (s, 2H), 3.03 (m, 2H), 1.63 (m, 2H), 1.42 (m, 2H), 1.36 (s, 9H); ^{13}C NMR (100 MHz, $CDCl_3$) δ 162.9, 155.8, 113.0, 78.7, 66.4, 39.9, 29.3, 28.1, 27.7, 24.4, 22.7; IR (film) ν_{max} 3367, 2929, 1746, 1695, 1249, 1167; HRMS calc for $C_{13}H_{22}N_2O_4Na$ $(M+Na)^+$ 293.1472 found 293.1473.

β-Cyanoacetate 20c. 74% yield; yellow oil; R_f 0.4 (2% MeOH in CH_2Cl_2); ^{1}H NMR (400 MHz, $CDCl_3$) δ 4.69 (bs, 1H), 4.09 (m, 2H), 3.42 (s, 2H), 3.00 (bs, 2H), 1.59 (m, 2H), 1.39–1.27 (m, 15H); ^{13}C NMR (100 MHz, $CDCl_3$) δ 162.9, 155.8, 113.0, 78.6, 66.5, 40.1, 29.6, 28.1, 27.9, 26.0, 25.1, 24.4; IR (film) ν_{max} 3367, 2935, 1746, 1691, 1248, 1163; HRMS calc for $C_{14}H_{24}N_2O_4Na$ $(M+Na)^+$ 307.1628 found 307.1630.

β-Cyanoacetate 20d. 48% yield; yellow oil; R_f 0.39 (2% MeOH in CH_2Cl_2); ^{1}H NMR (400 MHz, $CDCl_3$) δ 4.57 (bs, 1H), 4.16 (t, 2H, J = 6.4 Hz), 3.44 (s, 2H), 3.05 (m, 2H), 1.63 (m, 2H), 1.40 (s, 10H), 1.27 (s, 9H); ^{13}C NMR (100 MHz, $CDCl_3$) δ 162.9, 155.9,

113.0, 78.9, 66.9, 40.4, 29.9, 28.9, 28.9, 28.3, 28.1, 26.5, 25.5, 24.6; IR (film) ν_{max} 3367, 2979, 1746, 1692, 1248, 1164; HRMS calc for $C_{16}H_{28}N_2O_4Na$ $(M+Na)^+$ 335.1941 found 335.1943.

General procedure for the synthesis of carbamate 21. To a round bottom flask, compounds **17** (1.24 mmol) and **20** (1.24 mmol) were dissolved in dry THF (10 ml). To that, DBU (1.44 mmol) was added and the solution was left stirring at room temperature. Upon completion, the crude solution was concentrated under reduced pressure and the product was purified *via* flash chromatography (10–30% EthOAc–hexanes).

Carbamate 21a. 79% yield; yellow solid; R_f 0.41 (2% MeOH in CH_2Cl_2); ^1H NMR (400 MHz, $CDCl_3$) δ 8.03 (s, 1H), 7.44 (bs, 1H), 6.11 (d, 1H, $J = 4.6$ Hz), 4.83 (bs, 1H), 4.30 (t, 2H, $J = 6.1$ Hz), 3.45 (m, 4H), 3.23 (m, 2H), 1.90 (m, 2H), 1.71 (m, 6H), 1.44 (s, 9H); ^{13}C NMR (100 MHz, $CDCl_3$) δ 169.5, 165.3, 155.9, 146.4, 144.0, 119.8, 118.4, 104.9, 79.1, 62.7, 51.2, 37.3, 29.2, 28.4, 25.0, 23.5; IR (film) ν_{max} 2201, 1703, 1264; HRMS calc for $C_{21}H_{29}N_3O_4SNa$ $(M+Na)^+$ 442.1771 found 442.1776.

Carbamate 21b. 95% yield; yellow solid; R_f 0.60 (2% MeOH in CH_2Cl_2); ^1H NMR (400 MHz, $CDCl_3$) δ 8.03 (s, 1H), 7.44 (s, 1H), 6.10 (d, 1H, $J = 4.6$ Hz), 4.55 (bs, 1H), 4.22 (t, 2H, $J = 6.6$ Hz), 3.45 (m, 4H), 3.12 (m, 2H), 1.71 (m, 6H), 1.57 (m, 6H), 1.44 (s, 9H); ^{13}C NMR (100 MHz, $CDCl_3$) δ 169.3, 165.2, 146.4, 119.9, 118.5, 104.7, 94.3, 65.2, 51.2, 40.4, 29.7, 28.4, 28.4, 25.1, 23.5, 23.2; IR (film) ν_{max} 2923, 2201, 1703, 1240, 1193, 1069; HRMS calc for $C_{23}H_{33}N_3O_4SNa$ $(M+Na)^+$ 470.2084 found 470.2086.

Carbamate 21c. 70% yield; yellow solid; R_f 0.59 (2% MeOH in CH_2Cl_2); ^1H NMR (400 MHz, $CDCl_3$) δ 8.03 (s, 1H), 7.44 (bs, 1H), 6.10 (d, 1H, $J = 4.6$ Hz), 4.53 (bs, 1H), 4.21 (t, 2H, $J = 6.7$ Hz), 3.44 (m, 4H), 3.11 (m, 2H), 1.71 (m, 6H), 1.57 (s, 6H), 1.44 (m, 11H); ^{13}C NMR (100 MHz, $CDCl_3$) δ 169.2, 165.1, 155.9, 146.2, 143.6, 119.7, 118.4, 104.7, 78.8, 65.2, 51.1, 40.4 29.8, 28.5, 28.3, 26.3, 25.5, 24.9, 23.4; IR (film) ν_{max} 2201, 1704, 1247, 1198; HRMS calc for $C_{24}H_{35}N_3O_4SNa$ $(M+Na)^+$ 484.2240 found 484.2239.

Carbamate 21d. 73% yield; yellow solid; R_f 0.60 (2% MeOH in CH_2Cl_2); ^1H NMR (400 MHz, $CDCl_3$) δ 8.03 (s, 1H), 7.44 (bs, 1H), 6.10 (d, 1H, $J = 2.6$ Hz), 4.52 (bs, 1H), 4.21 (t, 2H, $J = 6.2$ Hz), 3.45 (bs, 4H), 3.10 (m, 2H), 1.71 (s, 6H), 1.57 (m, 6H), 1.44 (s, 9H), 1.32 (m, 6H); ^{13}C NMR (100 MHz, $CDCl_3$) δ 169.2, 165.2, 155.9, 146.3, 143.5, 119.9, 118.4, 104.7, 86.3, 78.9, 65.4, 51.2, 40.6, 30.0, 29.7, 29.1, 28.7, 28.4, 26.7, 25.8; IR (film) ν_{max} 2201, 1703, 1264, 1069; HRMS calc for $C_{26}H_{39}N_3O_4SNa$ $(M+Na)^+$ 512.2553 found 512.2552.

General procedure for the synthesis of ratiometric dye 23. A TFA solution was prepared by combining 5 ml of TFA with 0.1 ml of anisole in 4.9 ml of DCM. 2.76 ml of this solution were added to **21** (0.286 mmol) and the reaction was left stirring at room temperature. After 30 min, the reaction was completed and the solution was concentrated, rinsed with toluene (4 × 10 ml), concentrated, and dried under high vacuum to yield **22**. To a round bottom flask containing **22** dissolved in dry DCM (2 ml); DMAP (0.029 mmol), **9** (0.272 mmol), and DIPEA (0.572 mmol) were added. The reaction was left stirring at room temperature and monitored by TLC. Upon completion, the reaction was concentrated under reduced pressure and purified *via* flash chromatography (10–20% EtOAc–hexanes).

Dye 23a. 61% yield; orange solid; R_f 0.51 (3% MeOH in CH_2Cl_2); ^1H NMR (400 MHz, $CDCl_3$) δ 8.90 (bs, 1H), 8.82 (s, 1H), 8.03 (s, 1H), 7.57 (d, 1H, $J = 8.7$ Hz), 7.43 (s, 1H), 6.92 (dd, 1H, $J = 2.3$ Hz, $J = 8.7$ Hz), 6.84 (d, 1H, $J = 2.3$ Hz), 6.09 (d, 1H, $J = 4.6$ Hz), 4.33 (t, 2H, $J = 6.2$ Hz), 3.90 (s, 3H), 3.58 (m, 2H), 3.43 (m, 4H), 2.05 (m, 2H), 1.69 (m, 6H); ^{13}C NMR (100 MHz, $CDCl_3$) δ 169.4, 165.1, 164.7, 162.3, 161.7, 156.6, 148.3, 146.4, 130.9, 119.8, 118.3, 114.7, 113.9, 112.4, 104.8, 100.3, 62.9, 56.0, 51.2, 36.8, 28.8, 25.0, 23.5; IR (film) ν_{max} 3344, 2940, 2201, 1703, 1441, 1240, 1193, 1178, 1017; HRMS calc for $C_{27}H_{27}N_3O_6SNa$ $(M+Na)^+$ 544.1513 found 544.1517.

Dye 23b. 63% yield; orange solid; R_f 0.53 (3% MeOH in CH_2Cl_2); ^1H NMR (400 MHz, $CDCl_3$) δ 8.84 (s, 1H), 8.78 (bs, 1H), 8.03 (s, 1H), 7.57 (d, 1H, $J = 8.7$ Hz), 7.44 (bs, 1H), 6.93 (dd, 1H, $J = 2.1$ Hz, $J = 8.7$ Hz), 6.86 (d, 1H, $J = 2.1$ Hz), 6.09 (d, 1H, $J = 4.5$ Hz), 4.24 (t, 2H, $J = 6.6$ Hz), 3.91 (s, 3H), 3.46 (m, 6H), 1.81–1.65 (m, 12H); ^{13}C NMR (100 MHz, $CDCl_3$) δ 169.2, 165.1, 164.7, 162.0, 156.6, 148.1, 146.3, 130.9, 118.3, 113.9, 112.5, 104.7, 100.3, 65.2, 56.0, 51.2, 39.6, 34.0, 29.1, 28.4, 25.0, 23.5, 23.4; IR (film) ν_{max} 2940, 2201, 1707, 1441, 1245, 1189, 1178, 1071; HRMS calc for $C_{29}H_{31}N_3O_6SNa$ $(M+Na)^+$ 572.1826 found 572.1823.

Dye 23c. 70% yield; orange solid; R_f 0.33 (100% ether); ^1H NMR (400 MHz, $CDCl_3$) δ 8.84 (s, 1H), 8.77 (bs, 1H), 8.03 (s, 1H), 7.58 (d, 1H, $J = 8.7$ Hz), 7.43 (bs, 1H), 6.93 (dd, 1H, $J = 2.3$ Hz, $J = 8.7$ Hz), 6.86 (d, 1H, $J = 2.3$ Hz), 6.09 (d, 1H, $J = 4.6$ Hz), 4.22 (t, 2H, $J = 6.7$ Hz), 3.91 (s, 3H), 3.45 (m, 6H), 1.79–1.63 (m, 10H), 1.45 (m, 4H); ^{13}C NMR (100 MHz, $CDCl_3$) δ 169.2, 165.2, 164.7, 161.9, 156.5, 148.1, 146.3, 130.9, 119.9, 118.4, 114.9, 113.9, 112.4, 104.6, 100.2, 65.3, 56.0, 51.2, 39.7 33.9, 31.6, 29.7, 29.3, 28.6, 26.7, 25.6, 25.0, 23.5, 22.6; IR (film) ν_{max} 2932, 2201, 1707, 1442, 1254, 1193, 1167, 1068; HRMS calc for $C_{30}H_{33}N_3O_6SNa$ $(M+Na)^+$ 586.1982 found 586.1979.

Dye 23d. 52% yield; orange solid; R_f 0.62 (2% MeOH in CH_2Cl_2); ^1H NMR (400 MHz, $CDCl_3$) δ 8.84 (s, 1H), 8.75 (bs, 1H), 8.03 (s, 1H), 7.58 (d, 1H, $J = 8.7$ Hz), 7.43 (bs, 1H), 6.93 (dd, 1H, $J = 2.2$ Hz, $J = 8.7$ Hz), 6.86 (d, 1H, $J = 2.2$ Hz), 6.09 (d, 1H, $J = 4.6$ Hz), 4.21 (t, 2H, $J = 6.7$ Hz), 3.91 (s, 3H), 3.44 (m, 6H), 1.70 (m, 10H), 1.36 (m, 8H); ^{13}C NMR (100 MHz, $CDCl_3$) δ 169.1, 165.2, 164.7, 161.9, 156.6, 148.1, 146.3, 130.9, 119.9, 118.4, 115.0, 113.9, 112.5, 104.7, 100.2, 65.5, 56.0, 51.2, 39.8, 29.4, 29.2, 29.1, 28.7, 26.9, 25.8, 25.0, 23.5; IR (film) ν_{max} 2930, 2201, 1710, 1445, 1264, 1198, 1070; HRMS calc for $C_{32}H_{37}N_3O_6SNa$ $(M+Na)^+$ 614.2295 found 614.2291.

General procedure for the synthesis of carbamate 25. To a solution of compound **24** (0.826 mmol) and **10** (0.826 mmol) in dry THF (5.4 ml), DBU (0.958 mmol) was added and left stirring at room temperature. Upon completion, the solution was concentrated under reduced pressure and the product was purified *via* flash chromatography (10–30% EtOAc–hexanes).

Carbamate 25a. 62% yield; dark orange solid; R_f 0.33 (2% MeOH in CH_2Cl_2); ^1H NMR (400 MHz, $CDCl_3$) δ 8.07 (s, 1H), 7.94 (d, 2H, $J = 9.1$ Hz), 6.70 (d, 2H, $J = 9.1$ Hz), 4.35 (t, 2H, $J = 6.1$ Hz), 3.27 (m, 2H), 3.12 (s, 6H), 1.94 (m, 2H), 1.44 (s, 9H); ^{13}C NMR (100 MHz, $CDCl_3$) δ 164.4, 155.9, 154.8, 153.6, 134.1, 119.2, 117.5, 111.5, 93.4, 79.2, 63.4, 40.0, 37.3, 29.0, 28.4; IR (film)

ν_{max} 3450, 2214, 1706, 1612, 1570, 1522, 1270, 1173; HRMS calc for $C_{20}H_{27}N_3O_4Na$ $(M+Na)^+$ 396.1894 found 396.1897.

Carbamate 25b. 72% yield; dark orange solid; R_f 0.40 (2% MeOH in CH_2Cl_2); ^1H NMR (400 MHz, $CDCl_3$) δ 8.01 (s, 1H), 7.89 (d, 2H, J = 9.1 Hz), 6.65 (d, 2H, J = 9.1 Hz), 4.64 (bs, 1H), 4.23 (t, 2H, J = 6.6 Hz), 3.13–3.06 (m, 8H), 1.73 (m, 2H), 1.52 (m, 2H), 1.45–1.40 (m, 11H); ^{13}C NMR (100 MHz, $CDCl_3$) δ 164.2, 155.9, 154.4, 153.4, 133.9, 119.1, 117.4, 111.3, 93.6, 78.8, 65.5, 40.2, 39.9, 29.5, 28.3, 28.1, 23.0; IR (film) ν_{max} 3446, 2932, 2211, 1707, 1568, 1521, 1088; HRMS calc for $C_{22}H_{31}N_3O_4Na$ $(M+Na)^+$ 424.2207 found 424.2209.

Carbamate 25c. 78% yield; dark orange solid; R_f 0.34 (EtOAc–hexanes 4 : 6); ^1H NMR (400 MHz, $CDCl_3$) δ 7.94 (s, 1H), 7.81 (d, 2H, J = 9.0 Hz), 6.58 (d, 2H, J = 9.0 Hz), 4.73 (bs, 1H), 4.17 (t, 2H, J = 6.5 Hz), 3.00 (m, 8H), 1.65 (m, 2H), 1.46–1.27 (m, 15H); ^{13}C NMR (100 MHz, $CDCl_3$) δ 164.0, 155.7, 154.1, 153.3, 133.7, 118.9, 117.2, 111.1, 93.3, 78.5, 65.5, 40.1, 39.7, 29.6, 28.2, 28.1, 26.1, 25.3; IR (film) ν_{max} 2933, 2203, 1706, 1571, 1521, 1270, 1063; HRMS calc for $C_{23}H_{33}N_3O_4Na$ $(M+Na)^+$ 438.2363 found 438.2366.

Carbamate 25d. 73% yield; dark orange solid; R_f 0.38 (EtOAc–hexanes 4 : 6); ^1H NMR (400 MHz, $CDCl_3$) δ 8.03 (s, 1H), 7.90 (d, 2H, J = 9.0 Hz), 6.66 (d, 2H, J = 9.0 Hz), 4.57 (bs, 1H), 4.23 (t, 2H, J = 6.7 Hz), 3.08 (s, 8H), 1.70 (m, 2H), 1.41 (m, 13H), 1.30 (m, 6H); ^{13}C NMR (100 MHz, $CDCl_3$) δ 164.2, 155.9, 154.4, 153.4, 133.9, 119.2, 117.4, 111.4, 93.8, 78.8, 65.8, 40.5, 39.9, 29.9, 29.0, 28.5, 28.3, 26.6, 25.7; IR (film) ν_{max} 3461, 2203, 1735, 1713, 1570, 1266, 1103; HRMS calc for $C_{25}H_{37}N_3O_4Na$ $(M+Na)^+$ 466.2676 found 466.2679.

General procedure for the synthesis of ratiometric dye 27. A TFA solution was prepared by combining 5 ml of TFA with 0.1 ml of anisole in 4.9 ml of DCM. 2.76 ml of this solution were added to **25** (0.286 mmol) and the reaction was left stirring at room temperature. After 30 min, reaction was completed and the solution was concentrated, rinsed with toluene (4 × 10 ml), concentrated again, and dried under high vacuum to yield compound **26**. To a round bottom flask containing **26** in dry DCM (2 ml), DMAP (0.029 mmol), **9** (0.272 mmol), and DIPEA (0.572 mmol) were added. The reaction was left stirring overnight at room temperature. Upon completion, the reaction was concentrated and purified *via* flash chromatography (10–20% ethyl acetate in hexane).

Dye 27a. 69% yield; orange solid; R_f 0.41 (2% MeOH in CH_2Cl_2); ^1H NMR (400 MHz, $CDCl_3$) δ 8.90 (bs, 1H), 8.83 (s, 1H), 8.07 (s, 1H), 7.92 (d, 2H, J = 9.0 Hz), 7.56 (d, 1H, J = 8.7 Hz), 6.92 (dd, 1H, J = 2.4 Hz, J = 8.7 Hz), 6.84 (d, 1H, J = 2.4 Hz), 6.67 (d, 2H, J = 9.0 Hz), 4.38 (t, 2H, J = 6.2 Hz), 3.91 (s, 3H), 3.61 (m, 2H), 3.11 (s, 6H), 2.09 (m, 2H); ^{13}C NMR (100 MHz, $CDCl_3$) δ 164.7, 164.3, 162.2, 161.8, 156.6, 154.7, 153.5, 148.2, 134.1, 130.9, 119.3, 117.4, 114.8, 114.0, 112.4, 111.4, 100.2, 93.7, 63.4, 56.0, 40.0, 36.7, 28.7; IR (film) ν_{max} 3349, 2208, 1706, 1612, 1557, 1522, 1173; HRMS calc for $C_{26}H_{25}N_3O_6Na$ $(M+Na)^+$ 498.1636 found 498.1638.

Dye 27b. 74% yield; orange solid; R_f 0.43 (2% MeOH in CH_2Cl_2); ^1H NMR (400 MHz, $CDCl_3$) δ 8.80 (bs, 2H), 8.03 (s, 1H), 7.90 (d, 2H, J = 9.1 Hz), 7.55 (d, 1H, J = 8.7 Hz), 6.91 (dd, 1H, J = 2.4 Hz, J = 8.7 Hz), 6.83 (d, 1H, J = 2.4 Hz), 6.65 (d, 2H, J = 9.1 Hz), 4.27 (t, 2H, J = 6.6 Hz), 3.89 (s, 3H), 3.47 (m, 2H), 3.08 (s, 6H), 1.79 (m, 2H), 1.69 (m, 2H), 1.52 (m, 2H); ^{13}C NMR (100 MHz, $CDCl_3$) δ 164.6, 164.2, 162.0, 161.8, 156.5, 154.5, 153.5, 148.1, 134.0, 130.8, 119.3, 117.4, 114.7, 113.9, 112.4, 111.4, 100.2, 93.8, 65.6, 55.9, 39.9, 39.5, 29.0, 28.2, 23.3; IR (film) ν_{max} 3349, 2213, 1717, 1570, 1523, 1167; HRMS calc for $C_{28}H_{29}N_3O_6Na$ $(M+Na)^+$ 526.1949 found 526.1950.

Dye 27c. 64% yield; orange solid; R_f 0.43 (2% MeOH in CH_2Cl_2); ^1H NMR (400 MHz, $CDCl_3$) δ 8.83 (bs, 1H), 8.77 (s, 1H), 8.05 (s, 1H), 7.92 (d, 2H, J = 9.0 Hz), 7.57 (d, 1H, J = 8.7 Hz), 6.92 (dd, 1H, J = 2.2 Hz, J = 8.7 Hz), 6.84 (d, 1H, J = 2.2 Hz), 6.67 (d, 2H, J = 9.0 Hz), 4.26 (t, 2H, J = 6.6 Hz), 3.90 (s, 3H), 3.45 (m, 2H), 3.09 (s, 6H), 1.76 (m, 2H), 1.65 (m, 2H), 1.46 (m, 4H); ^{13}C NMR (100 MHz, $CDCl_3$) δ 164.7, 164.3, 161.9, 161.8, 156.5, 154.5, 153.5, 148.1, 134.0, 130.8, 119.3, 117.4, 114.8, 113.9, 112.4, 111.4, 100.2, 94.0, 65.8, 56.0, 40.0, 39.7, 29.3, 28.5, 26.6, 25.6; IR (film) ν_{max} 3349, 2214, 1713, 1616, 1567, 1525, 1167; HRMS calc for $C_{29}H_{31}N_3O_6Na$ $(M+Na)^+$ 540.2105 found 540.2103.

Dye 27d. 78% yield; orange solid; R_f 0.34 (EtOAc–hexanes 1 : 1); ^1H NMR (400 MHz, $CDCl_3$) δ 8.81 (s, 1H), 8.75 (bs, 1H), 8.03 (s, 1H), 7.91 (d, 2H, J = 9.0 Hz), 7.56 (d, 1H, J = 8.7 Hz), 6.91 (dd, 1H, J = 2.3 Hz, J = 8.7 Hz), 6.84 (d, 1H, J = 2.3 Hz), 6.66 (d, 2H, J = 9.0 Hz), 4.24 (t, 2H, J = 6.7 Hz), 3.89 (s, 3H), 3.43 (m, 2H), 3.08 (s, 6H), 1.72 (m, 2H), 1.60 (m, 2H), 1.36 (m, 8H); ^{13}C NMR (100 MHz, $CDCl_3$) δ 164.6, 164.3, 161.8, 161.8, 156.5, 154.4, 153.4, 148.0, 134.0, 130.8, 119.3, 117.4, 114.8, 113.9, 112.4, 111.4, 100.2, 93.9, 65.9, 55.9, 40.0, 39.7, 29.3, 29.1, 29.1, 28.5, 26.9, 25.7; IR (film) ν_{max} 3356, 2214, 1713, 1570, 1525, 1370, 1176; HRMS calc for $C_{31}H_{35}N_3O_6Na$ $(M+Na)^+$ 568.2418 found 568.2415.

Ratiometric dye 28. To a round bottom flask containing compound **26a** (0.669 mmol) (prepared as described for the synthesis of **27**) dissolved in dry DCM (5.6 ml); DMAP (8 mg, 0.067 mmol), **9** (213 mg, 0.736 mmol), and DIPEA (0.2 ml, 1.339 mmol) were added and left stirring overnight at room temperature. Upon completion, the reaction was concentrated under reduced pressure and purified *via* flash chromatography (0–7% MeOH–DCM) to yield dye **28** (163 mg, 53%). **28**: red solid; R_f 0.33 (3% MeOH in CH_2Cl_2); ^1H NMR (400 MHz, DMSO-d_6) δ 8.74 (bs, 2H), 8.04 (s, 1H), 7.87 (d, 2H, J = 9.1 Hz), 7.76 (d, 1H, J = 8.6 Hz), 6.84 (dd, 1H, J = 2.1 Hz, J = 8.6 Hz), 6.76 (d, 2H, J = 9.1 Hz), 6.73 (d, 1H, J = 2.1 Hz), 4.28 (t, 2H, J = 6.1 Hz), 3.46 (m, 2H), 3.07 (s, 6H), 1.94 (m, 2H); ^{13}C NMR (100 MHz, DMSO-d_6) δ 163.9, 163.7, 161.9, 161.1, 156.4, 154.1, 153.8, 148.0, 133.8, 132.0, 118.2, 117.6, 114.5, 113.6, 111.7, 111.1, 101.9, 92.1, 64.0, 36.6, 28.3; IR (film) ν_{max} 3201, 2211, 1709, 1567, 1522, 1168; HRMS calc for $C_{25}H_{23}N_3O_6Na$ $(M+Na)+$ 484.1479 found 484.1481.

Ratiometric dye 29. In a round bottom flask, containing **10** (35 mg, 0.100 mmol) dissolved in DCM (0.85 ml), **26a** (38.0 mg, 0.100 mmol), DMAP (1 mg, 0.010 mmol), and DIPEA (40 µl, 0.200 mmol) were added. The reaction was left stirring at room temperature until completion, concentrated under reduced pressure and purified *via* flash chromatography (0.25–1% MeOH–DCM) to yield **29** (50 mg, 98%). **29**: yellow solid; R_f 0.42 (3% MeOH in CH_2Cl_2); ^1H NMR (400 MHz, $CDCl_3$) δ 8.85 (bs, 1H), 8.76 (s, 1H), 8.06 (s, 1H), 7.90 (d, 2H, J = 9.1 Hz), 7.63 (s, 1H),

Table 5 Solvent composition and viscosity

Pre-stained EG/EG/Gly volumes (ml)	Viscosity (mPa·s)	Log viscosity
0.5/0.5/4.0	414.4	2.617
0.5/1.0/3.5	276.0	2.441
0.5/1.5/3.0	183.9	2.265
0.5/2.0/2.5	122.5	2.088
0.5/2.5/2.0	81.6	1.912

6.89 (s, 1H), 6.66 (d, 2H, J = 9.1 Hz), 4.39 (t, 2H, J = 6.1 Hz), 4.00 (s, 3H), 3.62 (m, 2H), 3.11 (s, 6H), 2.09 (m, 2H); ^{13}C NMR (100 MHz, $CDCl_3$) δ 164.3, 161.8, 161.2, 159.6, 154.9, 154.7, 153.5, 147.1, 134.1, 129.8, 120.5, 119.3, 117.4, 116.0, 112.4, 111.4, 99.8, 93.7, 77.2, 63.5, 56.9, 40.0, 36.9, 28.6; IR (film) ν_{max} 3345, 2213, 1711, 1610, 1568, 1525, 1170; HRMS calc for $C_{26}H_{24}N_3O_6ClNa$ $(M+Na)^+$ 532.1246 found 532.1241.

General procedure for the determination of spectral properties. Each viscosity sample was mixed according to the volumes shown in the first column in Table 5 below. The viscosity of each sample was estimated by the summation of weighted ratio[32] of each solvent's viscosity at 25 °C from the 91st Edition of the CRC Handbook of Chemistry and Physics, 2010–2011. The glycerol (Gly) was heated to ensure more exact measuring during pipetting. The pre-stained ethylene glycol (EG) for each sample contained 100 μM of dye resulting in a final concentration of 10 μM for each sample. All samples were placed on rotating mixer for a minimum of 1 h before pouring into cuvettes for scanning. Preliminary fluorescent scanning was done on each dye dissolved in 414.4 mPa·s viscosity solvent to determine optimal excitation and peak emission and slit settings for each molecular rotor derivative. All fluorescent scanning was done in a Fluoromax-3 photon-counting spectrophotometer (Jobin–Yvon) with the temperature-controlled turret (Quantum Northwest) set at room temperature (25 °C). Each sample was inserted in the turret and allowed to equilibrate for 10 min before testing. The monochromator slit settings for all calculations were 3 nm. For each solvent the fluorescent emission in an 11 nm range around peak emission was averaged and the logarithm of the average peak intensity was plotted against the logarithm of the viscosity. The slope was obtained for each molecular rotor derivative by linear regression (Graphpad Prism 4.01, San Diego, CA). The exponent x of each viscosity gradient was used to evaluate viscosity sensitivity, with a higher value of the exponent x indicating higher sensitivity. R^2 values indicate the linear regression of the log-transformed data (intensity over viscosity).

Determination of ratiometric intensity in liposome model membranes. To determine the efficacy of the ratiometric dyes within a phospholipid bilayer, each rotor was incorporated into giant unilamellar vesicles following the previously described DLPC liposome electroformation protocol.[33] The ratiometric liposome batch was then separated into 2 groups with n = 10 independent repeats. The experimental group comprised of an equal parts liposome suspension and 5% propanol/sucrose solution, and the control group comprised of equal parts liposome suspension and pure sucrose solution. The samples were excited at 352 nm and fluorescence spectra were recorded using the Fluoromax spectrophotometer. Emissions for the reference and rotor peak were recorded at 410 nm and 480 nm, respectively. The ratiometric measurements were calculated by taking the peak rotor intensity divided by the peak reference intensity (eqn (3)). From paired propanol/control sets, a percent change in the ratiometric intensity as a consequence of propanol exposure was then computed and presented in Fig. 7.

Acknowledgements

Financial support from the National Institutes of Health (1R21 RR025358 and CA 133002) and the National Science Foundation (CMMI-0652476) is gratefully acknowledged. We thank the NSF for instrumentation grants CHE-9709183 and CHE-0741968. We also thank Dr A. Mrse and Dr Y. Su for NMR and MS assistance respectively.

Notes and references

1 (*a*) K. Luby-Phelps, *Int. Rev. Cytol.*, 2000, **192**, 189–221; (*b*) *Molecular and Cellular Aspects of Basement Membranes*, Academic, San Diego, CA, 1993; (*c*) *The Membranes of Cells* Academic, San Diego, CA, 1993; (*d*) *Membrane Abnormalities in Sickle Cell Disease and in other Red Blood Cell Disorders*, CRC, Boca Raton, FL, 1994.
2 (*a*) W. H. Reinhart, *Biorheology*, 2001, **38**, 203–212; (*b*) P. M. Moriarty and C. A. Gibson, *Cardiovasc. Rev. Rep.*, 2003, **24**, 321–325; (*c*) I. Uchimura and F. Numano, *Diabetes Frontier*, 1997, **8**, 33–37; (*d*) A. Simon, J. Gariepy, G. Chironi, J.-L. Megnien and J. J. Levenson, *J. Hypertens.*, 2002, **20**, 159–169.
3 (*a*) N. Oppenheimer and H. Diamant, *Biophys. J.*, 2009, **96**, 3041–3049; (*b*) D. M. Owen, D. Williamson, C. Rentero and K. Gaus, *Traffic*, 2009, **10**, 962–971; (*c*) M. Frick, K. Schmidt and B. Nichols, *Curr. Biol.*, 2007, **17**, 462–467.
4 O. G. Luneva, N. A. Brazhe, N. V. Maksimova, O. V. Rodnenkov, E. Y. Parsina, N. Y. Bryzgalova, G. V. Maksimov, A. B. Rubin, S. N. Orlov and E. I. Chazov, *Pathophysiology*, 2007, **14**, 41–46.
5 (*a*) J. S. Goodwin, K. R. Drake, C. L. Remment and A. K. Kenworthy, *Biophys. J.*, 2005, **89**, 1398–1410; (*b*) M. D. Dibner, K. A. Ireland, L. A. Koerner and D. L. Dexter, *Cancer Res.*, 1985, **45**, 4998–5003.
6 (*a*) A. M. Aleardi, G. Benard, O. Augereau, M. Malgat, J. C. Talbot, J. P. Mazat, T. Letellier, J. Dachary-Prigent, G. C. Solaini, R. Rossignol and J. Bioenerg, *J. Bioenerg. Biomembr.*, 2005, **37**, 207–225; (*b*) X. Hou, S. J. Richardson, M.-I. Aguilar and D. H. Small, *Biochemistry*, 2005, **44**, 11618–11627.
7 (*a*) J. H. Ahn, T. Y. Kim, Y.-J. Kim, M. W. Han, T. H. Yoon and J. W. Chung, *Diabetic Med.*, 2006, **23**, 1339–1343; (*b*) B. Y. Salazar Vazquez, M. A. Salazar Vasquez, V. C. Venzor, A. C. Negrete, P. Cabrales, J. S. Diaz and M. Intaglietta, *Clin. Hemorheol. Microcirc.*, 2008, **38**, 67–74.
8 A. Kearney-Schwartz, J. M. Virion, J.-F. Stoltz, P. Drouin and F. Zannad, *Fundam. Clin. Pharmacol.*, 2007, **21**, 387–396.
9 I. Velcheva, N. Antonova, V. Dimitrova, N. Dimitrov and I. Ivanov, *Clin. Hemorheol. Microcirc.*, 2006, **35**, 155–157.
10 G. J. C. G. M. Bosman, I. G. P. Bartholomeus and W. J. de Grip, *Gerontology*, 1991, **37**, 95–112.
11 International Committee for Standardization in Haematology, *J. Clin. Pathol.*, 1984, 37, pp. 1147–1152.
12 S. Wang, A. H. Boss, K. R. Kensey and R. S. Rosenson, *Clin. Chim. Acta*, 2003, **332**, 79–82.
13 J. R. Lakowicz, *Principles of Fluorescence Spectroscopy*, Springer, New York, NY, 3rd edn, 2006.
14 M. Shinitzky and Y. Barenholz, *Biochim. Biophys. Acta*, 1978, **515**, 367–394.
15 (*a*) D. Axelrod, D. E. Koppel, J. Schlessinger, E. Elson and W. W. Webb, *Biophys. J.*, 1976, **16**, 1055–1069; (*b*) D. M. Soumpasis, *Biophys. J.*, 1983, **41**, 95–97; (*c*) R. Swaminathan, S. Bicknese, N. Periasamy and A. S. Verkman, *Biophys. J.*, 1996, **71**, 1140–1151.
16 J. C. G. Blonk, A. Don, H. van Aalst and J. J. Birmingham, *J. Microsc.*, 1993, **169**, 363–374.
17 (*a*) M. A. Haidekker and E. A. Theodorakis, *Org. Biomol. Chem.*, 2007, **5**, 1669–1678; (*b*) P. Demchenko, Y. Mely, G. Duportail and A. S. Klymchenko, *Biophys. J.*, 2009, **96**, 3461–3470.

18 (*a*) M. A. Haidekker and E. A. Theodorakis, *J. Biol. Eng.*, 2010, **4**, 11; (*b*) Z. R. Grabowski, K. Rotkiewicz and W. Rettig, *Chem. Rev.*, 2003, **103**, 3899–4031.
19 J. Sutharsan, D. Lichlyter, N. E. Wright, M. Dakanali, M. A. Haidekker and E. A. Theodorakis, *Tetrahedron*, 2010, **66**, 2582–2588.
20 (*a*) Z.-C. Wen and Y.-B. Jiang, *Tetrahedron*, 2004, **60**, 11109–11115; (*b*) M. K. Kuimova, S. W. Botchway, A. W. Parker, M. Balaz, H. A. Collins, H. L. Anderson, K. Suhling and P. R. Ogilby, *Nat. Chem.*, 2009, **1**, 69–73.
21 M. A. Haidekker, M. E. Nipper, A. Mustafic, D. Lichlyter, M. Dakanali and E. A. Theodorakis, in *Advanced Fluorescence Reporters in Chemistry and Biology I. Fundamentals, and Molecular Design.*, ed. A. P. Demchenko, Springer-Verlag, 2010, pp. 267–308.
22 (*a*) M. A. Haidekker, T. P. Brady, D. Lichlyter and E. A. Theodorakis, *J. Am. Chem. Soc.*, 2006, **128**, 398–399; (*b*) D. Fischer, E. A. Theodorakis and M. A. Haidekker, *Nat. Protoc.*, 2007, **2**, 227–236.
23 T. Förster, *Ann. Phys.*, 1948, **437**, 55–75.
24 M. Kamiya, H. Kobayashi, Y. Hama, Y. Koyama, M. Bernardo, T. Nagano, P. L. Choyke and Y. Urano, *J. Am. Chem. Soc.*, 2007, **129**, 3918–3929.
25 Ø. W. Akselsen, L. Skattebøl and T. V. Hansen, *Tetrahedron Lett.*, 2009, **50**, 6339–6341.
26 (*a*) L. B. Poole, B.-B. Zeng, S. A. Knaggs, M. Yakubu and S. B. King, *Bioconjugate Chem.*, 2005, **16**, 1624–1628; (*b*) B. S. Creaven, D. A. Egan, K. Kavanagh, M. McCann, A. Noble, B. Thati and M. Walsh, *Inorg. Chim. Acta*, 2006, **359**, 3976–3984; (*c*) T. Berthelot, J.-C. Talbot, G. Laïn, G. Déleris and L. Latxague, *J. Pept. Sci.*, 2005, **11**, 153–160.
27 D. Prim, G. Kirsch and J.-F. Nicoud, *Synlett*, 1998, 383–384.
28 C. E. Wheelock, *J. Am. Chem. Soc.*, 1959, **81**, 1348–1352.
29 (*a*) W.-C. Sun, K. R. Gee and R. P. Haugland, *Bioorg. Med. Chem. Lett.*, 1998, **8**, 3107–3110; (*b*) B. Abrams, Z. Diwu, O. Guryev, S. Aleshkov, R. Hingorani, M. Edinger, R. Lee, J. Link and T. Dubrovsky, *Anal. Biochem.*, 2009, **386**, 262–269.
30 H. V. Ly and M. L. Longo, *Biophys. J.*, 2004, **87**, 1013–1033.
31 (*a*) M. A. Haidekker, T. Ling, M. Anglo, H. Y. Stevens, J. A. Frangos and E. A. Theodorakis, *Chem. Biol.*, 2001, **8**, 123–131; (*b*) M. A. Haidekker, A. G. Tsai, T. Brady, H. Y. Stevens, J. A. Frangos, E. A. Theodorakis and M. Intaglietta, *Am. J. Physiol.-Heart C.*, 2002, **282**, H1609–H1614; (*c*) M. A. Haidekker, T. Brady, K. Wen, C. Okada, H. Y. Stevens, J. M. Snell, J. A. Frangos and E. A. Theodorakis, *Bioorgan. Med. Chem.*, 2002, **10**, 3627–3636; (*d*) M. A. Haidekker, T. P. Brady, S. H. Chalian, W. Akers, D. Lichlyter and E. A. Theodorakis, *Bioorg. Chem.*, 2004, **32**, 274–289; (*e*) M. A. Haidekker, T. P. Brady, D. Lichlyter and E. A. Theodorakis, *Bioorg. Chem.*, 2005, **33**, 415–425; (*f*) J. Sutharsan, D. M. Dakanali, C. C. Capule, M. A. Haidekker, J. Yang and E. A. Theodorakis, *ChemMedChem*, 2009, **5**, 56–60.
32 W. Akers, M. A. Haidekker and J. Biomech, *Eng.-Trans ASME.*, 2004, **126**, 340–345.
33 M. E. Nipper, S. Majd, M. Mayer, J. C.-M. Lee, E. A. Theodorakis and M. A. Haidekker, *Biochim. Biophys. Acta, Biomembr.*, 2008, **1778**, 1148–1153.

